WORLD JOURNAL OF PHARMACEUTICAL RESEARCH
SJIF Impact Factor 8.453
Volume 14, Issue 12, 826-844. Research Article ISSN 2277–7105

FORMULATION AND CHARACTERIZATION OF SIMVASTATIN NANOPARTICLES

Lingampalle Swapna*, K. Prathibha, Dr. Avinash Dundigalla and Dr. A. Yasodha.

Department of Pharmaceutics, Dhanvanthri College of Pharmaceutical Sciences, Tirumala hills, Appannapally, Mahabubnagar Telangana India 509001.

Article Received on
27 April 2025,

Revised on 17 May 2025,
Accepted on 07 June 2025

DOI: 10.20959/wjpr202512-37146

***Corresponding Author**
Lingampalle Swapna
Department of Pharmaceutics, Dhanvanthri College of Pharmaceutical Sciences, Tirumala hills, Appannapally, Mahabubnagar Telangana India 509001.

ABSTRACT

The aim of this study is to formulate and characterize simvastatin loaded Chitosan nanoparticles prepared by ionic-gelation method. simvastatin Calcium has a low bioavailability (20%) due to poor absorption of the drug. Chitosan is a polymer of linear polysaccharide, which enhances transport of drug across epithelial surfaces and is biocompatible and biodegradable. The nanoparticles obtained were evaluated for percentage yield of drug, drug entrapment efficiency, particle size and morphology using Scanning Electron Microscopy (SEM), compatibility studies using Fourier-Transform Infrared Spectroscopy (FTIR) and Differential Scanning Calorimetry (DSC) and in vitro release kinetics. Among the four different drug to polymer ratios, 1:1 ratio showed high encapsulation efficiency and drug loading. The nanoparticles obtained were spherical in shape with a smooth surface with particle size range between 231.52 ± 24.12 nm to 405.25 ± 17.42 nm. The nanoparticles prepared proved to be a promising dosage form of simvastatin, with improved bioavailability.

KEYWORDS: Simvastatin, Chitosan, Nanoparticles, Bioavailability, Ionic-Gelation.

INTRODUCTION

Simvastatin, bis[(E)-7-[4- (4-fluorophenyl)-6-isopropyl-2- [methyl(methylsulfonyl)amino] pyrimidin-5-yl](3R,5S)- 3,5-dihydroxyhept-6-enoic acid] salt is a member of the drug class of statins used to treat high cholesterol and related conditions and prevent cardiovascular disease. It acts by competitive inhibition of HMG-CoA reductase which is the rate controlling enzyme of the mevalonate pathway that produces cholesterol.[1,2]

The drug has a poor solubility and poor permeability which leads to low bioavailability (absolute bioavailability 20%).[3]

Since the dissolution and permeation are the rate limiting factors for the low bioavailability, it becomes a requirement to improve permeability and dissolution of drug. The major impediment allied to the use of many poorly soluble drugs is due to limited dissolution rate which results in poor absorption and low bioavailability. There are several strategies to improve solubility and enhance the dissolution rate and oral bioavailability of poorly soluble drugs e.g. inclusion complex[4], micronization[5], salt formation[6], solid dispersion[7] etc. These strategies often aim to increase the surface area, solubility, wettability of the drug.

Nanoparticles are nanoscale shells made out of a nontoxic polymer. They are made up of a polymeric membrane which encapsulates drug core in nanoscale level to form a vesicular system.[8,9] These colloidal particles have a diameter in the range of 10- 1000 nm. Nanoparticles have a myriad of uses.

Polymeric nanoparticles have been currently used as potential drug delivery system because of several advantages over the other techniques since the nano-sized structure of nanoparticles allows for the permeation through cell membranes[10], which makes them as an effective carrier of drug in biological systems to achieve improved bioavailability.[11] Similarly, oral route is the most accepted route of administration and hence the polymeric nanoparticles of the drug can be given by oral route.

Various methods have been proposed for the preparation of nanoparticles. Nanoprecipitation[12], Emulsion – Diffusion[13], Double emulsification[14], Emulsification Coacervation[15] and recently, the encapsulation technique used in medicine.

Many natural polymers gained importance in recent years for use in new drug delivery applications. The dissolution rate of drugs from the formulation containing viscous carriers is generally sustained due to the formation of gel layer on the hydrated surfaces. Chitosan polymer is a linear polysaccharide composed of randomly distributed β-(1-4)-linked D-glucosamine(deacetylated unit)and N-acetyl-D-glucosamine (acetylated unit) derived by deacetylation of chitin.[16] It gained great interest in pharmaceutical research because of its advantages like biocompatible, biodegradable, nonimmunogenic, nontoxic and low cost.[17]

Chitosan is insoluble in water, but can be dissolved in most of the organic acid solutions at pH less than 6.5 such as lactic acid, acetic acid, tartaric acid etc.[18] Such fibers might inhibit the uptake of dietary lipids.[19] Simvastatin is sparingly soluble in aqueous solutions and its solubility decreases with decrease in pH. The present study is aimed to increase the bioavailability of the drug by developing nanoparticles of Simvastatin using Chitosan by ionic gelation method.[20]

MATERIALS AND METHODS

Materials

Simvastatin (RC) was purchased from Hetero drugs, India. Chitosan (CS) was obtained from Novamatrix, Norway. Acetic acid, Sodium Tripolyphosphate (TPP), Diethyl ether, Trifluoroacetic acid, Dimethyl sulfoxide (DMSO), and Acetonitrile was procured from Sigma-Aldrich, USA. Poloxamer 188 was procured from BASF, Germany. Deionized water was obtained from a Millipore filtration system, USA.

Method of preparation of drug loaded nanoparticles

Nanoparticles of RC prepared using CS as a coating material by ionic gelation method[21] where the positively charged amino group in the CS interacts with negatively charged TPP to form coacervates with a size in the range of nanometer.

RC and CS were weighed in different ratios (1:0.25, 1:0.50, 1:0.75 and 1:1). CS was dissolved separately in an aqueous solution of Acetic acid (2% v/v) at pH 5.5. Poloxamer 188 (Poloxamer 188/CS ratio: 5/1) was dissolved in the above solution.[22]

RC was dissolved separately with DMSO (7.5% w/v of drug) and was added slowly to the above aqueous solution containing CS, while stirring under the magnetic stirrer.

Aqueous solution of TPP (CS/TPP ratio: 1/0.1) added in drops to the above solution, under magnetic stirring for 3 hrs at a speed of 1000 RPM (Remi Magnetic Stirrer MLH, India) resulted in cross linking of CS and TPP as depicted in **Fig 1** and produced the nanoparticles.

The above said process was captured in Fig 2

After 3 hours, nanoparticles formed were recovered by centrifugation (REMI cooling centrifuge, India) at 3000 rpm for 30 min. The nanoparticles recovered were washed using diethyl ether and lyophilized.

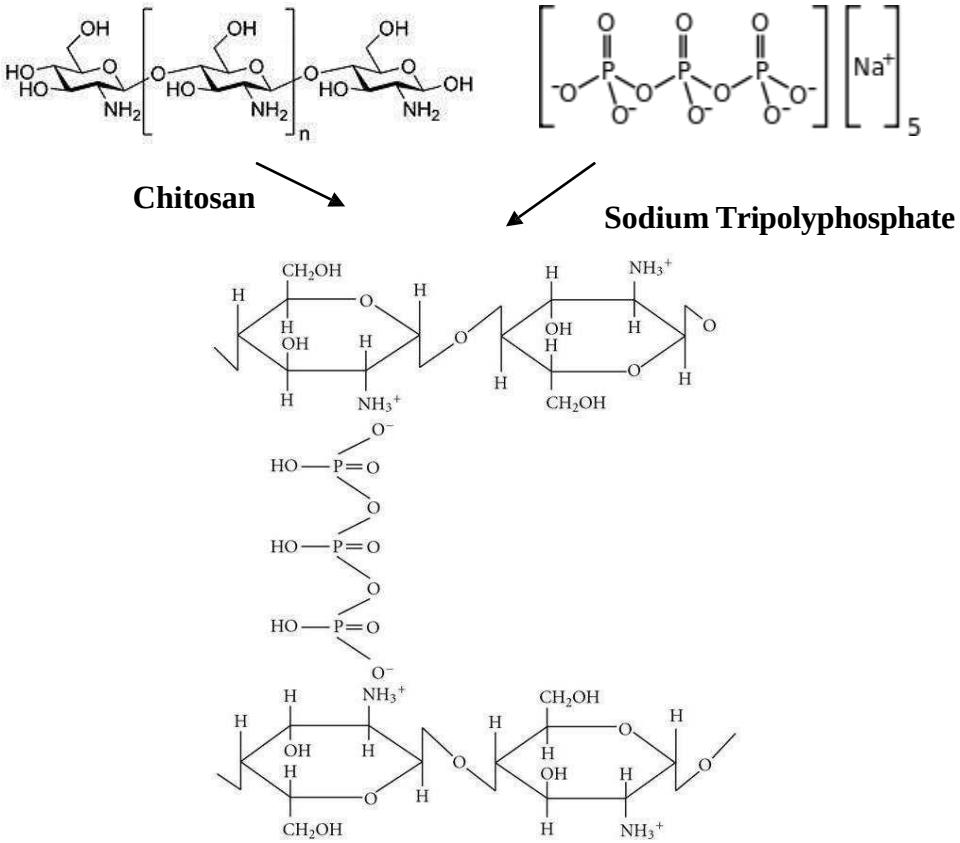

Fig. 1: Schematic of nanoparticle formation process by ionic gelation process. Chitosan forms a cross linking with Sodium Tripolyphosphate.

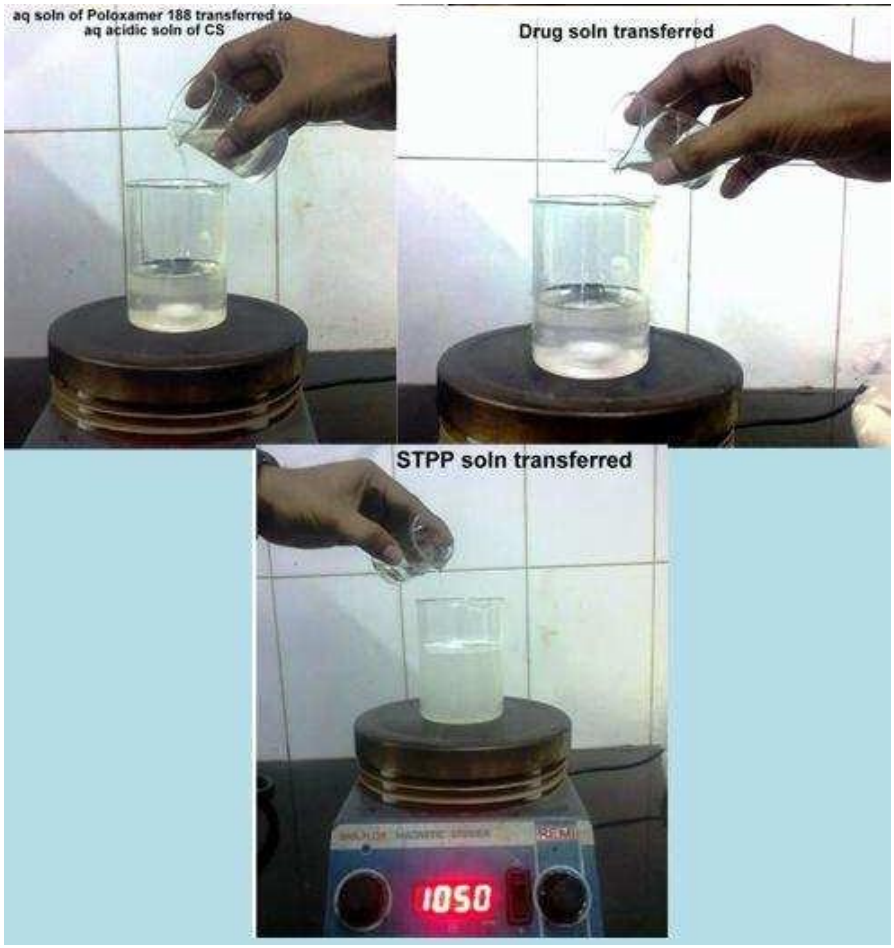

Fig. 2: Preparation of Simvastatin Nanoparticles. ***Stage by stage manufacturing process of Rosvastatin nanoparticles.***

Determination of nanoparticle yield, drug content and entrapment efficiency

The yield of nanoparticle (%) was calculated using equation (1).

$$\text{Nanoparticle Yield} = \left\{ \frac{\text{Mass of the Nanoparticle recovered}}{\text{Mass of drug, polymer and other excipients}} \right\} \times 100 \quad \ldots\ldots\ldots (1)$$

Drug Content and Entrapment Efficiency were determined using equation (2) and (3) respectively.

Nanoparticles equivalent to 5mg of drug were dissolved in 50mL mixture of Trifluoroacetic acid, Acetonitrile and Milli-Q Water in a ratio of 0.1:65.0:34.9. The solution was further diluted with the same mixture of solvents. Drug quantification was performed using HPLC (Waters HPLC system equipped with a quaternary pump, SIL-10AD auto injector, CTO-10A column oven and UV detector units) with a Sunfire™ column (C8 250mm x 4.6 mm, 5 µm).

The chromatographic conditions were injection volume = 50 µL, flow rate = 2.0 mL min^{-1} mobile phase = 0.1/65.0/34.9 of Trifluoroacetic acid/Acetonitrile/Milli-Q Water (pH 2.40). UV detection was performed at 210 nm.

All samples were measured in triplicate. The method was validated in terms of precision, accuracy, linearity, limit of detection (LOD), and limit of quantification (LOQ). The results were expressed as mean ± standard deviation.

$$\text{Drug Content (\%)} = \left\{ \frac{\text{Mass of the drug in Nanoparticle}}{\text{Mass of Nanoparticle recovered}} \right\} \times 100 \quad \ldots\ldots\ldots (2)$$

$$\text{Entrapment Efficiency (\%)} = \left\{ \frac{\text{Mass of the drug in Nanoparticle}}{\text{Mass of drug used in formulation}} \right\} \times 100 \quad \ldots\ldots\ldots (3)$$

Particle characterization

Particle size, polydispersity index and zeta potential of RC nanoparticles were measured using Malvern Zetasizer (Malvern Instruments, UK) by dynamic light scattering and Electrophoretic **light scattering principle**. The particle size analysis was performed at a scattering angle of 90°C at room temperature. The diameter was averaged from three parallel measurements and expressed as mean ± standard deviation.

SEM was used to examine the particle surface morphology and shape. The nanoparticles were coated in Sputter coater with a thin layer of gold in an argon gas environment (Cressington 108 Auto sputter coater, UK). Photographs were taken using FEI Quanta FEG 200, (FEI, USA) at room temperature.

Differential Scanning Calorimetry (DSC) interpretation

Thermograms of the RC and its nanoparticles were recorded on MettlerSTAR SW 9.01 instrument (Mettler Toledo, Switzerland). The analysis was carried out in nitrogen atmosphere by heating 2 to 3 mg of sample on an aluminum crimp pan, at heating rate of 10°C/min. The runs were made in triplicate.

Fourier Transform Infrared Radiation Measurements (FT-IR)

FT-IR analysis was carried out for pure drug and nanoparticles obtained by mixing with Potassium Bromide (KBr) by pellet method, after a baseline correction made with dried

potassium bromide to confirm the compatibility. The pellet was prepared to a pressure of about 5 x 10^6 Pa, in an evacuated die, to produce a clear transparent disc of diameter 2 cm and thickness 0.2 cm. The spectra were recorded at room temperature on Fourier transform spectrometer (Perkin-Elmer, USA) from 4000 cm^{-1} to 400 cm^{-1}.

Powder X-Ray diffraction (PXRD) study

Crystallinity study was carried out by comparing XRD spectrum of drug with nanoparticles using Siemens Diffractometer D5000 (Siemens, Germany) to check peak of drug in individual state and in nanoparticles. The data was recorded at 2θ range of 10°C to 60°C at time of 0.5 sec. The inter-planar distance (d) and relative intensity I/Io corresponding to 2θ value were reported and compared.

In vitro release study

The in vitro release study of RC loaded CS nanoparticles having highest entrapment efficiency was carried out using USP dissolution apparatus type II (paddle method). Nanoparticles equivalent to 5 mg of RC were loaded using 900 ml of citric acid buffer (pH 4) at a rotating speed of 50 rpm and 37□C ± 0.5□C were the sink conditions could be easily maintained. Samples were collected at specific time intervals. 2 ml of aliquot was collected during each sampling point and it was replaced with an equal volume of fresh buffer.

The amount of drug release was determined by HPLC method as described under the determination of drug loading in the nanoparticles.

The in vitro release data were analyzed using various kinetic models which includes, the zero-order kinetic model[23], the first-order kinetic model[24], the Higuchi model[25], the Hixson-Crowell model[26], the Korsmeyer-Peppas model[27], the Makoid Banakar model,[28] the Peppas Sahlin model,[29] the Weibull model,[30] the Baker Lonsdale model[31] the Hopfenberg model,[32] the Probit model[33,34] the Logistic model[35] the Quadratic model[36,37] the Gompertz model[38] The model, which gives the highest correlation coefficient (R^2) is considered as the best fit of release data.

RESULTS AND DISCUSSION

Determination of nanoparticle yield, drug content and entrapment efficiency

The nanoparticle yield was high with increase in drug to polymer ratio. Similarly, the drug content and the entrapment efficiency increase with increase in drug to polymer ratio (Table

1). As depicted in Fig 3, it was observed that increasing the amount of polymer results in better drug entrapment. From the entrapment efficiency, 1:1 ratio showed better yield compared to the other three ratios. The nanoparticle yield increases with increase in drug entrapment. Similarly, the low drug to polymer ratio of 1:0.25 reflected with low entrapment efficiency.

Table 1: Nanoparticle yield, drug content and entrapment efficiency of different batches of nanoparticles prepared.

Formulation trial code	Drug to polymer ratio	Nanoparticle yield^ (% ± SD)	Drug Content^ (% ± SD)	Entrapment Efficiency^ (% ± SD)
FT-001 to FT-003	1:0.25	64.05 ± 8.16	19.89 ± 8.73	15.67 ± 5.13
FT-004 to FT-006	1:0.50	70.97 ± 6.45	30.73 ± 4.32	33.67 ± 4.16
FT-007 to FT-009	1:0.75	74.52 ± 2.90	43.11 ± 1.64	58.67 ± 4.04
FT-010 to FT-012	1:1.00	95.40 ± 2.40	46.27 ± 0.79	92.67 ± 1.15

^Note: Values are mean of three consecutive trials with its Standard Deviation (SD)

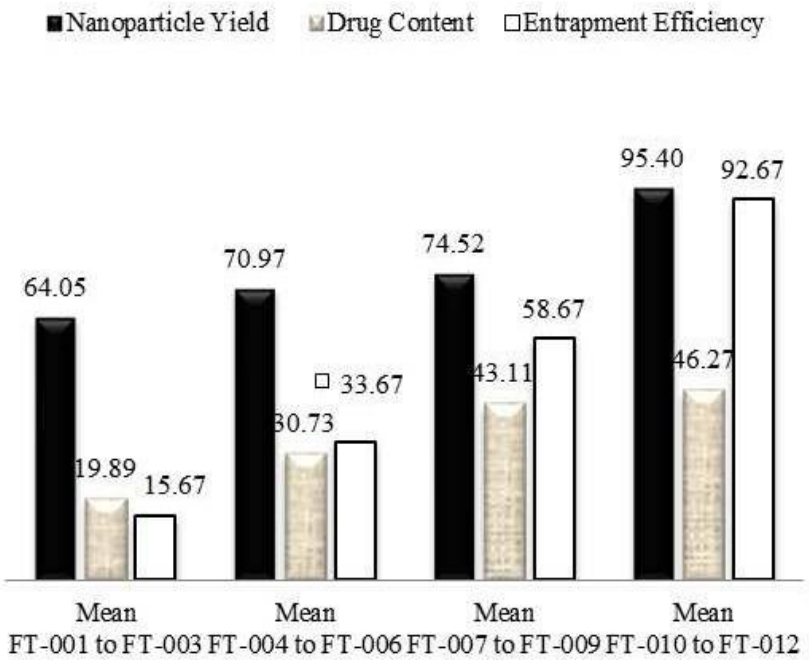

Fig. 3: Comparative results of nanoparticles yield, drug content and entrapment efficiency. *Trials taken with various ratios of Simvastatin and Chitosan.*

Particle characterization

The results indicate that the particle size increases with increase in concentration of CS. It was observed that the particle size of the RC loaded nanoparticles were between 231.52 ± 24.12 nm to 405.25 ± 17.42 nm.

Monodisperse samples have a lower Polydispersity Index value, whereas higher values of Polydispersity Index indicate a wider particle size distribution due to aggregation. The usual range of Polydispersity Index values is 0 to 0.05 for monodisperse standard, 0.05 to 0.08 for nearly monodisperse, 0.08 to 0.7 for mid range polydispersity and >0.7 for highly polydisperse.[39] The nanoparticles formulated had a Polydispersity Index of 0.245 ± 0.017 to 0.315 ± 0.023 as shown in Table 2 indicated mid range polydispersity. The addition of Poloxamer 188 aided in reducing the aggregation of nanoparticles which in turn was confirmed by the low Polydispersity Index of nanoparticles.

Zeta potential of prepared nanoparticles was found to be in the range between +26.8 ± 1.4 mV to +40.3 ± 1.6 mV. It was found that higher the zeta potential less will be the particle aggregation, due to electrostatic repulsion. The stability will be high if the Zeta Potential is high.

Table 2: Average Particle Size, Polydispersity index and Zeta Potential of nanoparticles prepared.

Drug to polymer ratio	Average Particle Size (nm)	Polydispersity index (D)	Zeta Potential (mv)
1:0.25	231.52 ± 24.12	0.315 ± 0.023	+26.8 ± 1.4
1:0.50	323.51 ± 18.58	0.301 ± 0.065	+29.6 ± 2.2
1:0.75	385.54 ± 22.15	0.275 ± 0.019	+34.8 ± 1.8
1:1.00	405.25 ± 17.42	0.245 ± 0.017	+40.3 ± 1.6

The microscopic imaging of SEM shown in the Fig 4 infers the surface morphology of RC nanoparticles with almost spherical surface, smooth and discrete nanoparticles.

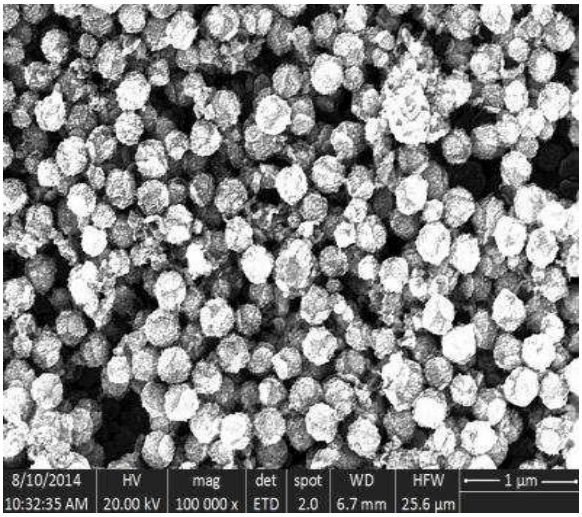

Fig. 4: Scanning Electron Microscopic imaging. ***Simvastatin nanoparticles observed under the scanning electron microscope.***

Determination of purity by Differential scanning colorimetry (DSC)

DSC thermograms of pure RC (Fig 5) showed a small endothermic peak at 140.45°C which closely corresponded to RC melting point. It also showed another endothermic peak at 232.45°C which corresponded to the degradation of RC.

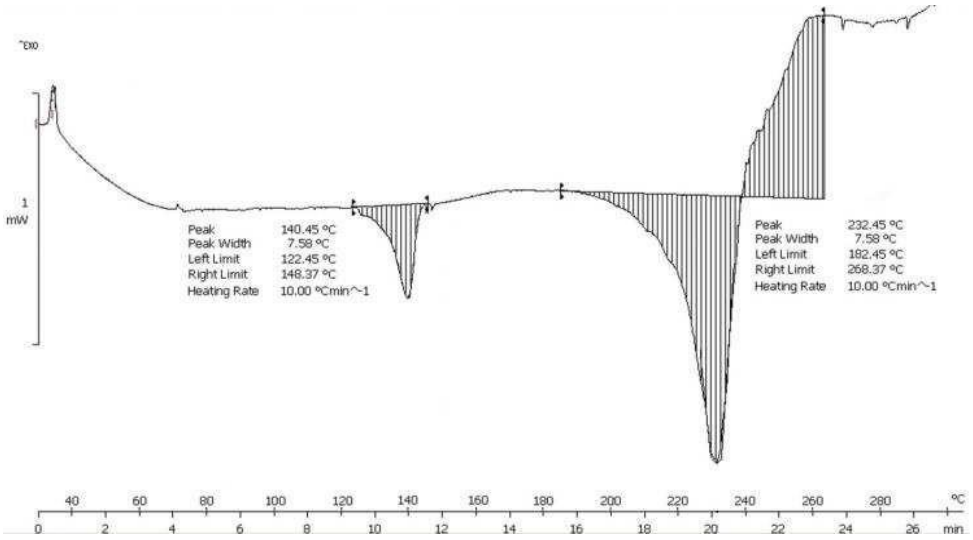

Fig. 5: DSC thermogram. ***The endothermic and exothermic peak of Simvastatin obtained using DSC.***

DSC thermogram of CS (Fig 6) showed a broad endothermic peak centered at about 93.45°C. This peak was attributed to the loss of water associated with the hydrophilic groups of the polymer due to evaporation.[40] This peak was observed even after drying the sample and keeping in the desiccators, before the analysis.

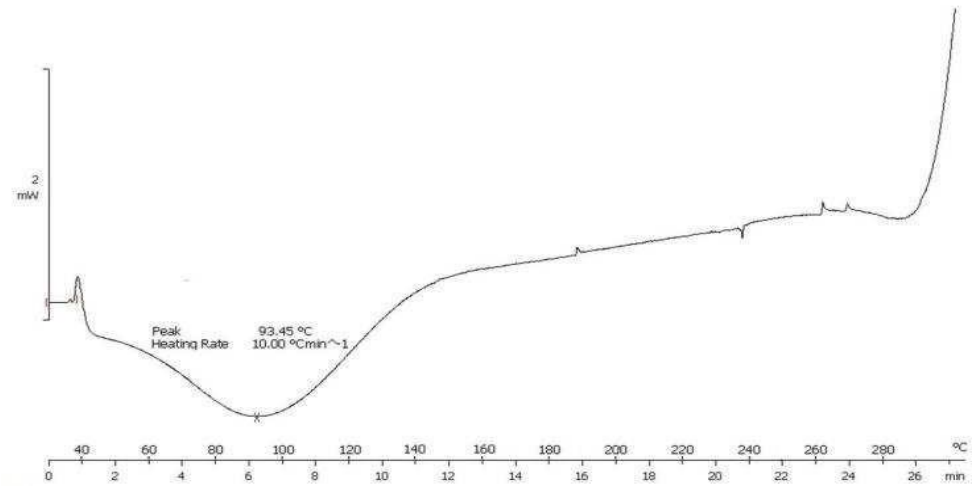

Fig. 6: DSC thermogram. ***The endothermic and exothermic peak of Chitosan obtained using DSC.***

The exothermic peak, which appeared in the temperature about 290°C, corresponded to the decomposition of the polymer.[41,42] The thermal degradation was due to the saccharide rings dehydration, depolymerization, decomposition of deacetylated and acetylated chitosan units.

After heating upto 150°C and holded for a minute, followed by cooling it upto 40°C, the moisture was removed and a second heating run was done, where it was found that the endothermic peak was not observed, which confirmed that this peak at around 93.45°C was due to water content in the sample. An exothermic peak was also observed due to degradation of chitosan as earlier mentioned.[43-45]

The RC nanoparticles showed an endothermic peak at 133.22°C. The slight shift in the peak of nanoparticles was due to incorporation of CS polymer. The results shown in Fig 7, clearly indicated compatibility between drug and polymer. There were no interactions observed in the obtained nanoparticles.

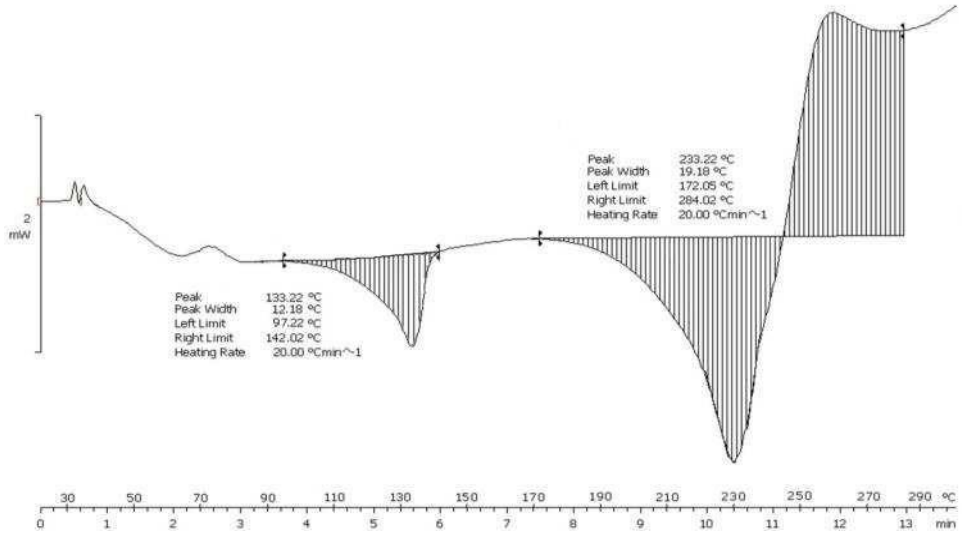

Fig. 7: DSC thermogram. ***The endothermic and exothermic peak of Simvastatin nanoparticles obtained using DSC.***

Determination of compatibility by Fourier transform infrared spectroscopy

The FT-IR spectrum of RC (Fig 8) revealed the characteristics peaks of 3392.14 cm^{-1} strong and broad band for carboxylic O- H stretching, 2967.91 cm^{-1} for C-H stretching, 2935.51 cm^{-1} for olefinic =C-H stretching, 1752.52 cm^{-1} for C=O stretching of carboxylic group, 1609.99 cm^{-1} for C=N stretching, 1547.59 cm^{-1} for C=C stretching, 1457.67 cm^{-1}, 1379.82 cm^{-1} and 776.21 cm^{-1} for asymmetric and symmetric bending vibration of C-H group respectively, 1320.12 cm^{-1} for C-N stretching, 1229.40 cm^{-1} for C-F stretching vibrations, 1174.19 cm^{-1}

represented the vibration for S=O, 965.20 cm^{-1} for aromatic C-H bending.

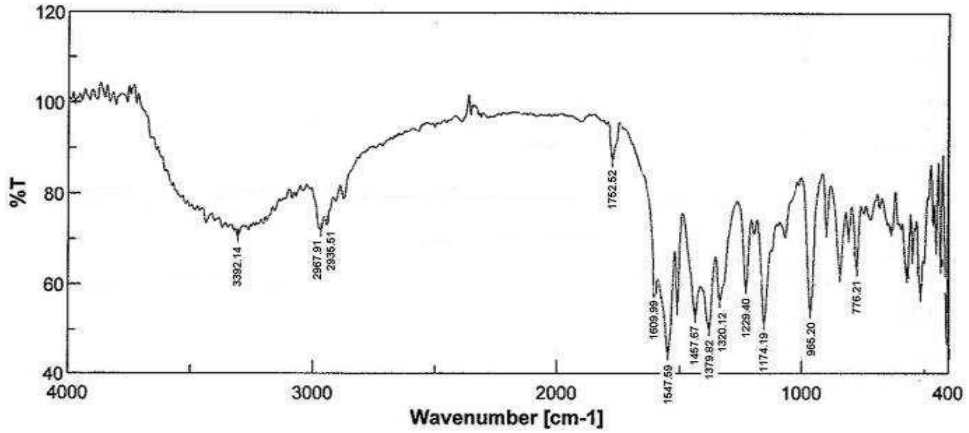

Fig. 8: FTIR spectrum. ***Finger print region between 4000cm^{-1} to 400cm^{-1} of Simvastatin.***

The FT-IR spectrum of CS (Fig 9) revealed the characteristic peaks of 3407.13 cm^{-1} for amine N-H symmetric vibration, 2915.54 cm^{-1} and 2887.54 cm^{-1} for C-H stretching, 1645.65 cm^{-1} for C-C stretching, 1558.25 cm^{-1} for amino group vibration, 1158.19 cm^{-1} and 905.53 cm^{-1} corresponded to saccharide structure of chitosan. The broad peak at 1050.91 cm^{-1} indicated C-O stretching vibration.[46,47]

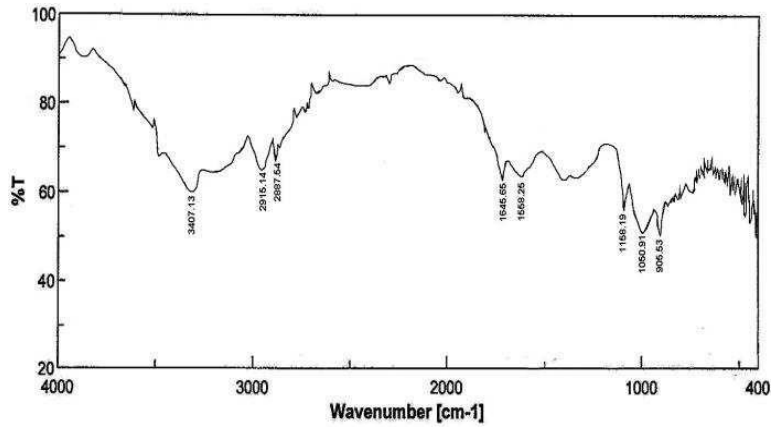

Fig. 9: FTIR spectrum. ***Finger print region between 4000cm^{-1} to 400cm^{-1} of Chitosan.***

The FT-IR spectrum of the final nanoparticles (Fig 10) revealed the presence of characteristic peaks of RC with a negligible shift which included 3402.26 cm^{-1} for broad O-H stretching vibration, 2985.76 cm^{-1} for C-H stretching, 2955.45 cm^{-1} for olefinic =C- H stretching, 1735.96 cm^{-1} C=O stretching of carboxylic group, 1345.85 cm^{-1} C-N stretching, 1220.47 cm^{-1} for C-F stretching, 1185.57 cm^{-1} for S=O group.

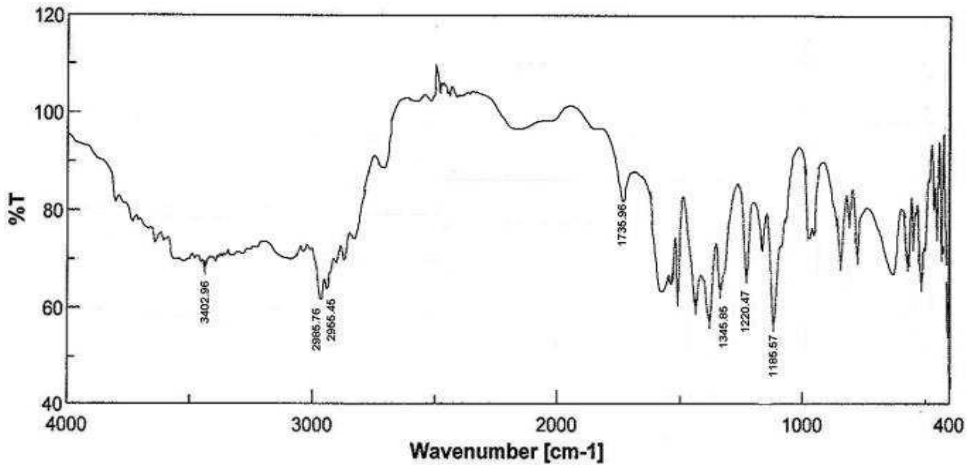

Fig 10. FTIR spectrum. ***Finger print region between 4000cm^{-1} to 400cm^{-1} of Simvastatin nanoparticles.***

From the above spectrum, it is clear that there were no incompatibilities present with the any of the added excipients.

Determination of crystallinity by X-ray diffraction study

PXRD was used to determine the crystallinity of compounds. Polymorphic changes of drug was an important factor, which might affect the dissolution rate and in turn bioavailability. Crystallinity of the drug and the nanoparticles was determined. The XRD pattern (Fig 11) of pure drug showed a broad diffraction peaks at 2θ as the drug is amorphous. Similarly nanoparticles also did not show any sharp peak at 2θ. This shows there was no formation of crystals in the resulted nanoparticles.

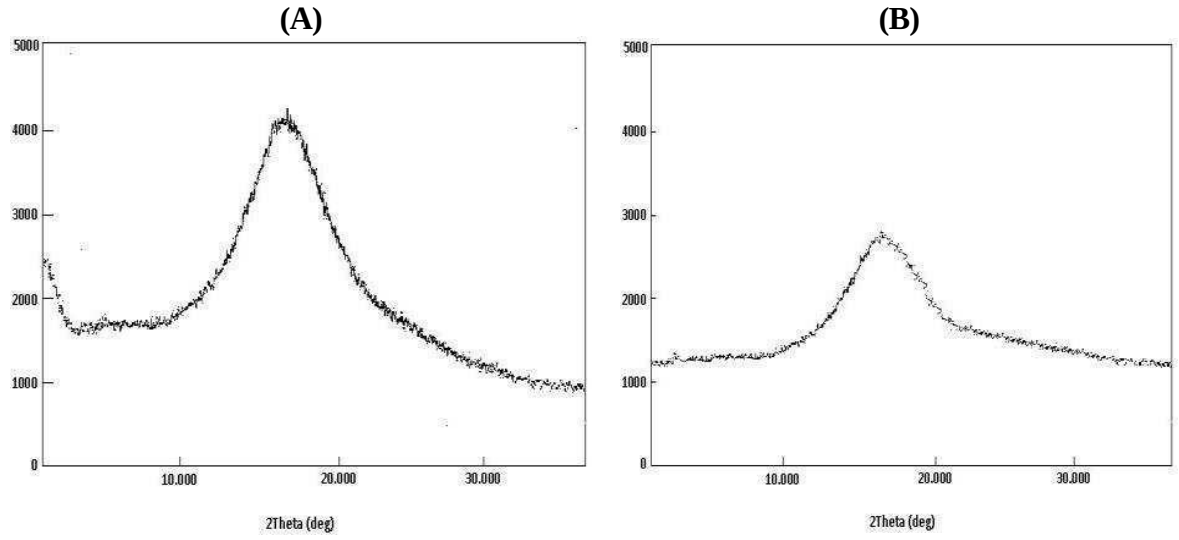

Fig. 11: XRD Study ***(A) Simvastatin showing no sharp peak (B) Simvastatin nanoparticles showing no sharp peak.***

In-vitro release studies and release profile

RC nanoparticles prepared with CS in a ratio of 1:1 (FT010, FT011 and FT012) were taken for dissolution since it had the highest entrapment efficiency when compared to other ratios. As shown in Fig 12, nanoparticles showed an initial burst release of around 18% RC in the first hour. This initial rapid release, characterized as ―burst effect‖, is due to the fact that some amounts of RC were localized on the surface of nanoparticles by adsorption which could be released easily by diffusion. After this initial burst effect, a slower sustained release occurred throughout the dissolution period.

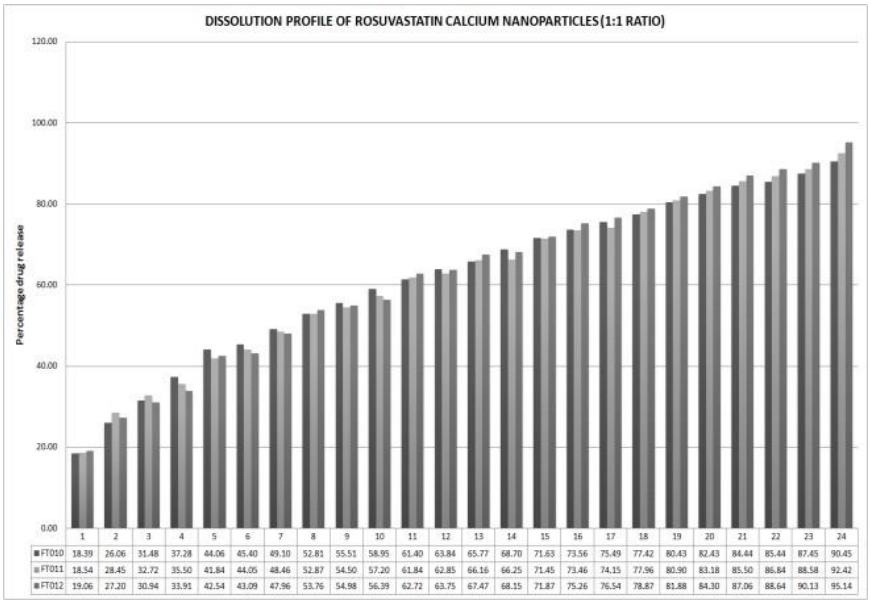

Fig. 12: Dissolution profile of Simvastatin nanoparticles. ***Dissolution profile of nanoparticles prepared using 1:1 ratio of Simvastatin and Chitosan in citric acid buffer solution (pH 4).***

Table 3 demonstrates correlation values (R2) and release parameters determined from the results of model fitting of the release profiles. According to the correlation values it fitted to Makoid Banakar, Peppas-Sahlin, Korsmeyer-Peppas and Higuchi models, which indicated that RC is released by diffusion. Moreover, the Korsmeyer-Peppas release model (high correlation values) exponent, *n*, is about 0.5066, which showed the characteristics of anomalous kinetics (non-Fickian), suggesting that more than one mechanism may be involved in release kinetics, referring to combination of diffusion and erosion based drug release mechanism. This mechanism could result from an increased plasticization at the relaxing boundary. The release data of the Hixson-Crowell model suggested that there is no change in surface area as a function of time.

Table 3: Mathematical Models and Correlation values (R^2) based on release data.

S No	Mathematical Model	Correlation Value (R^2)
1	Makoid Banakar	0.9986
2	Peppas-Sahlin	0.9986
3	Korsmeyer Peppas	0.9983 (n=0.5066)
4	Higuchi	0.9982
5	Weibull	0.9933
6	Baker Lonsdale	0.9607
7	First Order	0.9565
8	Hopfenberg	0.9565
9	Probit	0.9492
10	Logistic	0.9485
11	Quadratic	0.9207
12	Hixson Crowell	0.9150
13	Gompertz	0.9082
14	Zero Order	0.6107

CONCLUSION

RC loaded CS nanoparticles were successfully prepared by ionic gelation method in four different ratios 1:0.25, 1:0.50, 1:0.75 & 1:1. According to efficiency of yield and entrapment, 1:1 ratio showed better yield compared to other 3 ratios. The entrapment efficiency was found in the range of 15.67 ± 5.13% to 92.67 ± 1.15%. Average size of prepared nanoparticles varied from 231.52 ± 24.12 nm to 405.25 ± 17.42 nm with a polydispersity index in the range of 0.245 ± 0.017 to 0.315 ± 0.023. As the amount of polymer increased, size of the nanoparticles also increased. It was found that higher the zeta potential, lesser the particle aggregation and resulted in more stability of nanoparticles. DSC and FTIR completely suggested the drug to polymer compatibility. In-vitro release study showed sustained release of drug from 1:1 ratio of polymer upto 24 hours following diffusion and erosion based drug release mechanism. From the present study, it is concluded that RC loaded CS nanoparticles is an effective carrier for the design of controlled drug delivery of poor water soluble drug like RC.

Abbreviations

1. % - Percentage
2. °C - Degree Centigrade
3. cm - Centimeter
4. HPLC - High Performance Liquid Chromatography
5. mg - milligram
6. min - minute
7. ml - milliliter

8. mm - millimeter
9. mV - millivolts
10. nm - nanometer
11. Pa - Pascal
12. rpm - Revolutions per minute
13. SD - Standard Deviation
14. sec - second
15. UK - United Kingdom
16. USA - United States of America
17. UV - Ultra Violet
18. v/v - volume by volume
19. w/v - weight by volume

REFERENCES

1. Mc Taggart F, Buckett L, Davidson R, Holdgate G, McCormick A, Schneck D, et al. Preclinical and clinical pharmacology of Simvastatin, a new 3-hydroxy-3-methylglutaryl coenzyme A reducatase inhibitor. Am J Cardiol, 2001; 87(5A): 28B-32B.
2. Smith G, Davidson R, Bloor S, Burns K, Calnam CC, Aulay PMC, et al. Pharmacological properties of ZD4522 – a new HMG- CoA reductase inhibitor. Atherosclerosis Supplements, 2000; 151: 39.
3. Agarwal, RK; Showkathali, R. ―Simvastatin in acute coronary syndromes‖. Expert Opinion on Pharmacotherapy, June 2013; 14(9): 1215-1227.
4. Leuner C, Dressman J. Improving drug solubility for oral delivery using solid dispersions. Eur J Pharm Biopharm., 2000; 50: 47–60.
5. Kim, M.-S., Lee, S., Park, J.-S., Woo, J.-S., Hwang, S.-J. Micronization of cilostazol using supercritical antisolvent (SAS) process: effect of process parameters.Powder Technol., 2007; 177: 64–70.
6. Han, H.-K., Choi, H.-K. Improved absorption of meloxicam via salt formation with ethanolamines. Eur. J. Pharm. Biopharm., 2007; 65: 99–103.
7. Leuner C, Dressman J. Improving drug solubility for oral delivery using solid dispersions. Eur J Pharm Biopharm., 2000; 50: 47–60.
8. Kumaresh S. Soppimath, Tejraj M. Aminabhavi, Anandrao R. Kulkarni, Walter E. Rudzinski. Biodegradable polymeric nanoparticles as drug delivery devices. J Control Release, 2001; 70: 1–20.

9. Mohanraj VJ, Y Chen Nanoparticles – A Review. Trop J Pharm Res., 5(1): 561-573.
10. Schipper N, Olsson S, Hoogstrate J, de Boer A, Varum K, Artursson P. Chitosans as absorption enhancers for poorly absorbable drugs. 3: Influence of mucus on absorption enhancement. Eur J Pharm Sci., 1999; 8: 335-343.
11. Peer D, Karp J.M, Hong S, Farokhzad O.C, Margalit R, Langer R, Nanocarriers as an emerging platform for cancer therapy. Nat. Nanotechnol, 2007; 2: 761–770.
12. Claudia Elizabeth Mora-Huertas, Olivier Garrigues, Hatem Fessi, Abdelhamid Elaissari Nanocapsules prepared via nanoprecipitation and emulsification–diffusion methods: Comparative study, January 2012; 80(1): 235–239.
13. Quintanar-Guerrero D, Allémann E, Doelker E, Fessi H. Preparation and characterization of nanocapsules from preformed polymers by a new process based on emulsification-diffusion technique, Jul. 1998; 15(7): 1056-1062.
14. Bilati U, Allémann E, Doelker E. Sonication parameters for the preparation of biodegradable nanocapsules of controlled size by the double emulsion method. Pharm Dev Technol, 2003; 8(1): 1-9.
15. V. Deepa, R Sridhar, A Goparaju, P Neelakanta Reddy, P Balakrishna Murthy, Nanoemulsified ethanolic extract of Phyllanthus amarus Schum and ameliorates CCl_4 induced hepatotoxicity in Wistar rats, Indian Journal of Experimental Biology, November 2012; 50: 785–794.
16. Joseph BristoW, Chitosan manufacturing process, Nov 27, 2012 USPTO, US8318913 B2
17. Ghosh. PK Hydrophilic polymeric nanoparticles as drug carriers. Indian J Biochem Biophys, 2000; 37: 273-282.
18. Furda, Ivan. "Interaction of Dietary Fiber with Lipids — Mechanistic Theories and their Limitations". New Developments in Dietary Fiber. Advances in Experimental Medicine and Biology, 1990; 270: 67–82.
19. Ikeda, Ikuo.; Sugano, Michihiro.; Yoshida, Katsuko.; Sasaki, Eiji.; Iwamoto, Yasushi.; Hatano, Kouta. "Effects of chitosan hydrolyzates on lipid absorption and on serum and liver lipid concentration in rats". Journal of Agricultural and Food Chemistry, 1993; 41(3): 431–435.
20. Gouda, M., Elayaan, U. and Youssef, M.M. Synthesis and Biological Activity of Drug Delivery System Based on Chitosan Nanocapsules. Advances in Nanoparticles, 2014; 3: 148-158.
21. Ramkumar Ponnuraj et al. Formulation And Characterization of Epigallocatechin Gallate Nanoparticles. Indo American Journal of Pharm Research, 2015; 5(01).

22. Pena Ana Isabel Vila, Luque Silvia Suarez, Fernandez Ma Jose Alonso, Chitosan and heparin nanoparticles, 19 Apr 2007, WO2007042572 A1
23. T. P. Hadjiioannou, G. D. Christian, M. A. Koupparis, and P. E. Macheras,Quantitative Calculations in Pharmaceutical Practice and Research, VCH Publishers, New York, NY, USA, 1993.
24. D. W. A. Bourne, ―Pharmacokinetics,‖ in Modern Pharmaceutics, G. S. Banker and C. T. Rhodes , Eds., pp. 67–93, Marcel Dekker, New York, NY, USA, 2002.
25. T. Higuchi, ―Mechanism of sustained-action medication. Theoretical analysis of rate of release of solid drugs dispersed in solid matrices,‖ Journal of Pharmaceutical Sciences, 1963; 52: 1145–1149.
26. W. Hixson and J. H. Crowell, ―Dependence of reaction velocity upon surface and agitation,‖ Industrial & Engineering Chemistry, 1931; 23: 923–931.
27. R. W. Korsmeyer, R. Gurny, and E. Doelker, ―Mechanisms of solute release from porous hydrophilic polymers,‖ International Journal of Pharmaceutics, 1983; 15(1): 25–35.
28. Makoid MC, Dufour A, Banakar UV. Modelling of dissolution behaviour of controlled release systems. STP Pharma., 1993; 3: 49–58.
29. Peppas NA, Sahlin JJ. A simple equation for the description of solute release III. Coupling of diffusion and relaxation. Int J Pharm., 1989; 57: 169–72.
30. Langenbucher F. Linearization of dissolution rate curves by the Weibull distribution. J Pharm Pharmacol, 1972; 24: 979–81.
31. Baker RW, Lonsdale HS. Controlled release of biologically active agents. New York: Plenum, 1974.
32. Enscore DJ, Hopfenberg HB, Stannett VT. Effect of particle size on the mechanism controlling n-hexane sorption in glassy polystyrene microspheres. Polymer, 1977; 18: 793–800.
33. Sathe PM, Tsong Y, Shah VP. In-vitro dissolution profile comparison: statistics and analysis, model dependent approach. Pharm Res., 1996; 13: 1799–803.
34. Tsong Y, Hammerstrom T, Chen JJ. Multipoint dissolution specification and acceptance sampling rule based on profile modeling and principal component analysis. J Biopharm Stat., 1997; 7: 423–39.
35. Sathe PM, Tsong Y, Shah VP. In-vitro dissolution profile comparison: statistics and analysis, model dependent approach. Pharm Res., 1996; 13: 1799–803.
36. Polli JE, Rekhi GS, Augsburger LL, Shah VP. Methods to compare dissolution

profiles and a rationale for wide dissolution specifications for metoprolol tartrate tablets. J Pharm Sci., 1997; 86: 690–700.

37. Costa P, Sousa Lobo JM. Modeling and comparison of dissolution profiles. Eur J Pharm Sci., 2001; 13: 123–33.
38. Tsong Y, Hammerstrom T, Chen JJ. Multipoint dissolution specification and acceptance sampling rule based on profile modeling and principal component analysis. J Biopharm Stat., 1997; 7: 423–39.
39. Wolfgang S. Sample preparation in Light Scattering from Polymer Solutions and Nanoparticle Dispersions. Springer Berlin Heidelberg GmbH & Co. K., 2007; 43-44.
40. Cheung, M. K.; Wan, K. P. Y.; Yu P. H. J. Appl. Polym. Sci., 2002; 86: 1253-1258. & Gonzalez, V.; Guerrero, C.; Ortiz U. J. Appl. Polym. Sci., 2000; 78: 850-857.
41. Sakurai, K.; Maegawa, T.; Takahashi, T. Polymer., 2000; 41: 7051-7056.
42. Zeng, M.; Fang, Z.; Xu C. J. Membr. Sci., 2004; 230: 175-181.
43. Mathew S, Brahmakumar M, Abraham TE: Microstructural imaging and characterization of the mechanical, chemical, thermal, and swelling properties of starch-chitosan blend films. Biopolymers, 2006; 82-176.
44. Sarmento B, Ribeiro A, Veiga F, Ferreira D: Development and characterization of new insulin containing polysaccharide nanoparticles. Colloids Surf B Biointerfaces, 2006; 53-193.
45. Sankalia MG, Mashru RC, Sankalia JM, Sutariya VB: Reversed chitosan–alginate polyelectrolyte complex for stability improvement of alpha-amylase: optimization and physicochemical characterization. Eur J Pharm Biopharm, 2007; 65: 215-232.
46. de Souza Costa-Júnior E., Pereira M. M., Mansur H. S., Properties and biocompatibility of chitosan films modified by blending with PVA and chemically crosslinked, J. Mater. Sci.: Mater. Med., 2009; 20: 553–561.
47. Krishna Rao K.S.V., Vijaya Kumar Naidu B., Subha M.C.S., Sairam M., Aminabhavi T.M., Novel chitosan-based pH- sensitive interpenetrating network microgels for the controlled release of cefadroxil, Carbohydrate Polymers, 2006; 66: 333–344.